Gd^{3+} vibronic side band spectroscopy

New optical probe of Ca^{2+} binding sites applied to biological macromolecules

I. E. T. Iben,*‡ M. Stavola,§ R. B. Macgregor,‡ X. Y. Zhang,* and J. M. Friedman*

*Chemistry Department, New York University, New York, New York 10003; ‡AT&T Bell Laboratories, Murray Hill, New Jersey 07974; §Physics Department, Lehigh University, Bethlehem, Pennsylvania 18015 USA

ABSTRACT A new spectroscopic technique is presented for obtaining infraredlike spectra of the binding sites of Ca^{2+} and other metals in biological macromolecules. The technique, based on the Ca^{2+}-like binding properties of Gd^{3+}, utilizes vibronic side bands (VSB) that appear in Gd^{3+} fluorescence. In the fluorescence spectrum of Gd^{3+}, the separation in photon frequency[1] between a VSB and its electronic origin at $\sim$32,150 cm^{-1} ($\sim$311 nm) is a direct measure of the vibrational frequency of a ligand coordinated to Gd^{3+} ion. As a consequence, the VSB are uncomplicated by molecular vibrations distant from the Gd^{3+} binding site. The vibrational spectra resulting from the VSB of Gd^{3+} coordinated to a Ca^{2+} binding protein, a phospholipid, and DNA are presented.

INTRODUCTION

The functional and conformational properties of many biological macromolecules are modulated by site specific binding of Ca^{2+} ions. Because the Ca^{2+} ion has a closed outer shell, it cannot be directly probed by traditional optical or spin resonance spectroscopies (1). Information about the local environment of Ca^{2+} binding sites has been obtained by substituting it with spectroscopically active lanthanide ions, Ln^{3+} (1–3; see the Discussion for further references to the use of Ln^{3+} ions in biology). Because of the similarity between the ionic radii of Ln^{3+} and Ca^{2+}, many enzymes retain normal catalytic activity upon replacement of Ca^{2+} by Ln^{3+}, despite the difference in charge. Such results provide the basis for making the Ln^{3+} studies functionally relevant. Measurements of the fluorescence yields and lifetimes of Ln^{3+} ions bound to Ca^{2+} binding proteins have provided information on the number of water molecules at Ca^{2+} binding sites (3, 4), and the number of Ca^{2+} binding sites and their binding constants (1, 3–5). Förster energy transfer to or from Ln^{3+} ions coordinated to Ca^{2+} binding sites have yielded information on distances between binding sites and molecular groups (3, 4). Ln^{3+} ions have been used to induce membrane fusion (6), to study Ln^{3+} binding sites and their binding constants (7, 8), and to measure electrostatic surface potentials (8) in lipid membranes.

Though yielding valuable information, the above mentioned studies do not readily yield either the identity or structural properties of the molecular groups coordinated to the metal ion. Though Raman and infrared spectroscopies can, in principal, identify the coordinating molecules through the use of difference measurements, (spectra versus ion concentration), these techniques are not specific to the metal ion binding sites. In this work, a new probe of Ca^{2+} binding sites in biological macromolecules is demonstrated for the first time and evaluated for more widespread application.

It has been known for several decades that, in addition to sharp 4f $\rightarrow$ 4f electronic features, (or zero phonon lines, ZPL), the absorption and luminescence spectra of certain trivalent lanthanide ions coordinated with molecular groups show weak vibronic sidebands, (VSB) (9, 10). VSB, which are a result of short-range, dipole–dipole interactions that weakly couple the 4f electronic and ligand vibrational states (11–13), reflect the vibrational frequencies of the ligands. These VSB provide an opportunity to measure the vibrational spectra of ligands coordinated to lanthanide ion. The technique has previously been used as a probe of the local environment of lanthanide ions in aqueous solutions (14), organic solvents (15), and glasses (16).

Whereas it has been suggested that the VSB might provide a structure sensitive probe of metal ion binding sites in biological systems (11, 14, 15), recent studies have been unsuccessful because these relatively weak vibronic features have been obscured by background luminescence and Raman scattering as well as competition between strong molecular absorptions by biological molecules in the UV. We have overcome the above mentioned difficulties in three major classes of biological materials: proteins, lipids, and DNA with a time

Address correspondence to Dr. Friedman.

[1]In order to be consistent with standard vibrational spectroscopic terminology, the term frequency, and the units of wavenumbers (centimeter^{-1}) are used for energy. To convert from cm^{-1} to s^{-1}, multiply by 3×10^{10} cm s^{-1}. To convert from cm^{-1} to eV, multiply by 1.25×10^{-4} eV cm.

0006-3495/91/05/1040/10 $2.00

gated detector with a pulsed excitation source. Local vibrational spectra, that are not congested with contributions from the vibrations of the solvent or macromolecular material outside the immediate environment of the lanthanide ion have been determined directly.

It has been shown (5, 17–19) that changes in the local environment surrounding lanthanide ions result in shifts in the electronic absorption and emission spectra. This sensitivity raises the prospect of combining site selectivity with the VSB technique. Such shifts in the electronic spectrum make it possible to preferentially excite lanthanides at distinct binding sites. Such site selectivity, when combined with VSB spectroscopy, makes it possible to measure the vibrational spectra of distinct binding sites. The ability to measure a vibrational spectrum localized to the neighborhood of a specific ion is reminicent of resonance Raman techniques (20) which have proved extremely useful for measuring localized vibrational spectra in complicated biological systems. The combination of a local vibrational spectroscopy with site selectivity makes the VSB technique a promising probe of complex biological structures.

Gd^{3+} has several characteristics that make it best suited for the luminescence studies of vibronic sidebands that we report here. The energy gap ~32,100 cm^{-1} (21), between the lowest electronically excited state, $^6P_{7/2}$, above the ground state, $^8S_{7/2}$, minimizes the nonradiative quenching of luminescence (22). Because Gd^{3+} has no electronic energy levels between the $^8S_{7/2}$ and the $^6P_{7/2}$ states, the luminescence due to the $^6P_{7/2} \rightarrow {}^8S_{7/2}$ ZPL gives rise to an isolated electronic origin for the VSB. The VSB spectra of Tb^{3+}, on the other hand, is complicated by the existance of multiple electronic energy levels in close proximity to the ground state (11). Last, the excited state has a long lifetime, ~2 ms in aqueous solution (22), that permits effective discrimination against interferring luminescence and Raman processes with sensitive gate detectors (14) and provides a temporal window to probe dynamical processes that occur over time scales that are long compared to most fluorescent probes.

SAMPLES

The gadolinium used in these experiments was 99.999% pure $GdCl_3 \cdot 6H_2O$ salt purchased from Aldrich Chemical Co. (Milwaukee, WI). Doubly distilled H_2O was used. For hydrated Gd^{3+}, (5 mM), $GdCl_3 \cdot 6H_2O$ was dissolved in H_2O. Isatopically dilute HDO (3 M HDO in D_2O) was prepared by dissolving 0.5 M $GdCl_3 \cdot 6H_2O$ in >99.99% pure D_2O (Aldrich Chemical Co.). Ethylenediaminetetraacetic acid (EDTA) (99.5% pure from Aldrich Chemical Co.), was dissolved in H_2O with Gd^{3+}, buffered to pH 8 with Tris-HCl. Rabbit muscle parvalbumin (RMPA) (mol wt ~12,000) (23) was used as a representative calcium binding protein. RMPA was purchased from Sigma Chemical Co. (St Louis, MO). RMPA was dissolved in H_2O with $GdCl_3 \cdot 6H_2O$. The sample was then centrifuged through a 3,000 mol wt cutoff Centricon filter (Amicon Division of W. R. Grace and Co.-Conn., Danvers, MA) to a final concentration of 1 mM RMPA. The lipid dioleoylphosphatidylcholine (DOPC) was purchased from Avanti Polar Lipids, Inc. (Pelham, AL). A dried film of DOPC with GD^{3+} in a one-to-one ratio was prepared by dissolving $GdCl_3 \cdot 6H_2O$ in a solution of DOPC. Chloroform and methanol were added and the sample was placed on a quartz window to dry overnight. The effective concentration of Gd^{3+} was ~0.4 M. The dried film was then sealed with a second window. Calf-thymus DNA and the synthetic DNA poly$[d(A\text{-}T)]_2$ were purchased from Sigma Chemical Co. The DNA and Gd^{3+} were dissolved in water at low concentrations of both, and concentrated using a 30 K mol wt Centricon cutoff filter from Amicon Division of W. R. Grace and Co.-Conn. In the cases where the samples precipitated out of solution, the precipitate was loaded in the sample cell and some of the solution was added for thermal dissipation of the laser energy.

EXPERIMENTAL METHODS

For all spectra the excitation source was the frequency doubled light from an excimer pumped (EMG 101) tunable dye laser (FL 2002) from Lambda Physik (Götingen, FRG). The energy of the predoubled light was ~3 mJ per pulse and the laser repetition rate was 10 Hz. An Inrad autotracker II with a KDP doubling crystal was used to double the frequency of the output from the dye laser into the 32,150 cm^{-1} frequency range (~311 nm) for direct excitation of the lowest fluorescent energy level of Gd^{3+}, $^6P_{7/2}$ (16, 21) (Fig. 1). The UV excitation energy was ~0.3 mJ per pulse. This light was focused onto the front surface of the 1 mm thick samples that were loaded into a continuous flow dewar (R. G. Hansen and Associates, Santa Barbara, CA) for temperature

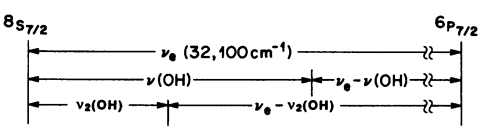

FIGURE 1 Simplified energy level diagram of hydrated Gd^{3+}. See Results for a detailed explanation.

control. The temperature of 80°K was used to help minimize nonradiative quenching of Gd^{3+} fluorescence. The back scattered light was collected with lenses and focused onto the entrance slit of a 1 M double spectrometer (U1000: Instruments SA, Metuchen, NJ). The light was dispersed by either 150 or 600 g/mm gratings. The dispersed light was detected by an intensified optical multichannel analyzer (OMA) (IRY OMA from Princeton Instruments; 1024 diodes, ~500 of which are intensified). The OMA was controlled with an ST-1000 controller (Princeton Instruments). Interference from Raman and fast fluorescence signals from the samples were eliminated by electronically gating the detector, i.e., turning the gain of the detector off until 5 μs (delay time, τ_d) after each excitation pulse. In all cases, the detector remained intensified for the following 6 ms (window time, τ_w). Thus, all photons within the 5 μs–6 ms window after the excitation pulse were collected. For the ZPL, the monochrometer slits were ≤20 μm and the accumulation times were 10 s. For the VSB, the monochrometer slits were ≤420 μm and the accumulation times were between 120 and 900 s. The spectrometer was calibrated using the lines from a mercury lamp. The excitation source was then calibrated using the spectrometer. The dispersion of the spectrometer at ~32,150 cm^{-1} is 8.24 and 2.06 cm^{-1} per diode using 150 and 600 g/mm gratings. The resolution of the detector is ~6 diodes (full widths at half maximum [fwhm]) or 50 and 12 cm^{-1} for the 150 and 600 g/mm gratings, respectively.

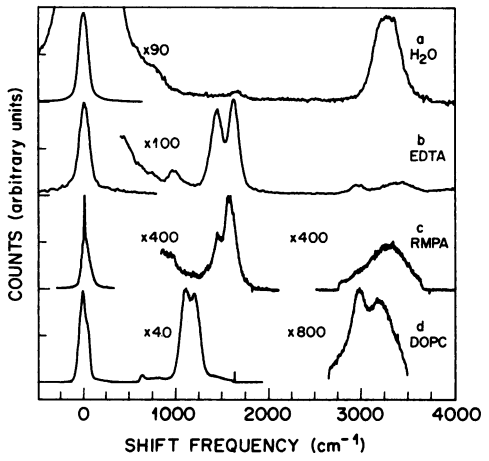

FIGURE 2 Fluorescence spectra of Gd^{3+} in four different coordinating environments. The data are all plotted in counts (arbitrary units) versus shift frequency as described in the text. (*a*) 0.5 M Gd^{3+} in H_2O at 80°K, ν_{exc} = 32,125 cm^{-1}. (*b*) 5 mM Gd^{3+} and 5 mM EDTA in H_2O at 80°K, ν_{exc} = 32,020 cm^{-1}. (*c*) 1 mM Gd^{3+} and 0.5 mM RMPA in H_2O at 80°K, ν_{exc} = 32,075 cm^{-1}. (*d*) ~0.4 M Gd^{3+} in a dried film of DOPC at 16°K, ν_{exc} = 32,075 cm^{-1}. The gratings used are 150 g/mm for *a* and *b* and 600 g/mm for *c* and *d*. The peaks at zero shift frequency for *b–d* are accumulations for 10 s with the entrance slit to the monochrometer open <10 μm. Accumulation times for the remainder of *b–d* are 300 s with the entrance slit open 400, 400, and 100 μm, respectively.

RESULTS AND ASSIGNMENTS

Vibronic sidebands, VSB

Fig. 1 shows a simplified energy level diagram of the ground and lowest-lying electronic excited state of Gd^{3+} with the vibrational frequencies of coordinated H_2O molecules (14, 16, 21, 23). This figure corresponds to the fluorescence emission spectrum shown in Fig. 2 *a*.The lowest excited fluorescent level of Gd^{3+},$^6P_{7/2}$, can be populated either by direct excitation (16) or by indirect excitation of the higher energy ^6I_j levels (14, 21) which nonradiatively decay to the $^6P_{7/2}$ level. Though the ^6I_j bands (21) have significantly larger absorption cross-sections, their excitation frequency of ~36,360 cm^{-1} (275 nm) coincides with strongly absorbing energy levels of the amino acids tyrosine and tryptophan and the base pairs of DNA. The fluorescence associated with the $^6P_{7/2} \rightarrow {}^8S_{7/2}$ ZPL of hydrated Gd^{3+} in water has a frequency, ν_{zpl}, peaked at ~32,125 cm^{-1}, with a fwhm of ~100 cm^{-1}. The ZPL and VSB in Fig. 2 *a* are plotted in photon intensity (arbitrary units) versus frequency shift from ν_{zpl}. Approximately 1% of the luminescing Gd^{3+} ions decay to a vibronic state in which the lanthanide ion is in its electronic ground state but in which the ligand is in a vibrationally excited state. These transitions result in a decrease in frequency of the emitted photons by the vibrational frequency of the coordinated H_2O molecules. The relative intensity of a given VSB is, to first order, proportional to its infrared (IR) active dipole moment (11, 24).[2] Because the VSB originate from dipole–dipole interactions between the Gd^{3+} ion and the coordinated molecules, the VSB transition probability falls off as R^{-6}, where R is the separation between the Gd^{3+} and the ligand. Thus, the VSB primarily reflect the vibrational levels of the molecules immediately coordinated to the Gd^{3+}.

H_2O; hydration layer

The shift frequencies of ~3,285 and ~1,645 cm^{-1}, respectively, represent the excitation of the OH stretch frequency, ν(OH), and the bending mode, ν_2(OH), of waters coordinated to Gd^{3+} (14, 25, 26). The high resolution spectrum of hydrated Gd^{3+} at 80°K reveals that ν(OH) is composed of two peaks, one at 3,185 cm^{-1} and another at 3,325 cm^{-1}. We assign them as the symmetric,

[2]This result uses several approximations which include ignoring the relative orientations of the Ln^{3+} and its coordinated molecules as well as neglecting any stark splitting of the j levels.

ν_s(OH), and antisymmetric, ν_a(OH), stretching modes of water, respectively. This assignment, though, is complicated by possible fermi resonance with $2\nu_2$(OH) and ν_a(OH) (26). These bands are crudely fit by two lorentzians with equal fwhm of $\sim$180 cm^{-1}. The relative intensity of the ν_s(OH) and ν_a(OH) bands change as the laser is tuned across the $^6P_{7/2}$ band, with ν_s(OH) being preferentially enhanced with red edge excitations. The positions and widths are insensitive to ν_{exc}. The spectrum of 3 M HDO in D_2O yields a single peak for ν(OH) centered at $\sim$3,305 cm^{-1} with a fwhm of $\sim$240 cm^{-1}.

EDTA: organic metal chelator

The peak ν_{zpl} for Gd^{3+} coordinated to EDTA is $\sim$32,020 cm^{-1} with a fwhm $\sim$60 cm^{-1}. The VSB spectra of Gd^{3+} coordinated to EDTA in H_2O, Figs. 2 *b* and 3 *a*, show two main peaks at shift frequencies of 1,425 and 1,600 cm^{-1} with fwhm $\sim$90 cm^{-1}. These bands are assigned as the symmetric and antisymmetric carbonyl stretches, ν_s(CO) and ν_a(CO) (15, 17, 27, 30). The shapes, positions, and relative intensities of the ν_s(CO) and the ν_a(CO) VSB from Gd^{3+} bound to EDTA are insensitive to ν_{exc}, and are unaffected when introduced into samples containing DNA or RMPA. Three peaks with much weaker intensities are measured at 980, 2,940, and 3,370 cm^{-1}. Using deuterated water as the solvent shifts the 3,370 cm^{-1} band to $\sim$2,465 cm^{-1} while not significantly altering the other bands. The D_2O insensitive 2,940 cm^{-1} band is therefore attributed to ν(CH) (28, 29), and the 3,370 cm^{-1} band is assigned to ν(OH).

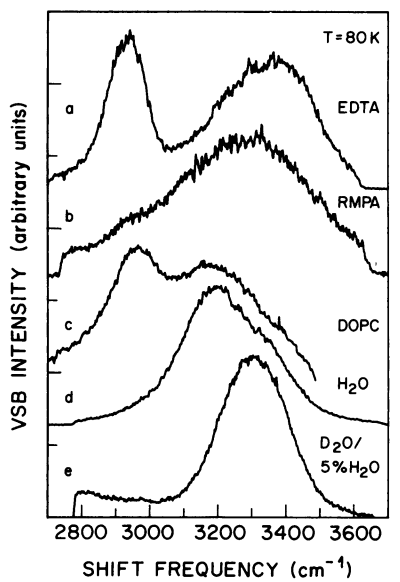

FIGURE 3 VSB fluorescent spectra of Gd^{3+} for the ν(OH) region in five different coordinating environments. 600 g/mm gratings, an entrance slit of 400 microns, a delay time of 5 μs, a window time of 6 ms, and an accumulation time of 300 s are used in all cases. (*a*) 5 mM Gd^{3+} and 15 mM EDTA dissolved in H_2O at 80°K, ν_{exc} = 32,050 cm^{-1}; (*b*) 1 mM Gd^{3+} and 0.5 mM RMPA dissolved in H_2O, ν_{exc} = 32,075 cm^{-1}; (*c*) dried film of 0.4 M Gd^{3+} and 0.4 M DOPC (see Fig. 2) at 16°K, ν_{exc} = 32,075 cm^{-1}; (*d*) 5 mM Gd^{3+} dissolved in H_2O, 80°K, ν_{exc} = 32,075 cm^{-1}; (*e*) 0.5 M $GdCl_3 \cdot 6H_2O$ dissolved in D_2O, (5.5% HDO by mole) ν_{exc} = 32,075 cm^{-1}.

RMPA: calcium binding protein

The ZPL of Gd^{3+} coordinated to RMPA is peaked at $\sim$32,075 cm^{-1} and has a fwhm of $\sim$100 cm^{-1}. The VSB spectra of 1 mM Gd^{3+} and 0.5 mM RMPA dissolved in H_2O are shown in Figs. 2 *c* and 3 *d*. The peak at $\sim$1,570 cm^{-1} and the shoulder at $\sim$1,460 cm^{-1} are respectively assigned to ν_s(CO) and ν_a(CO) from carbonyls. The shapes, positions, and relative intensities of the ν_s(CO) and ν_a(CO) bands are insensitive to ν_{exc}. The peak at the shift frequency of $\sim$3,280 cm^{-1} with a fwhm of $\sim$400 cm^{-1} is assigned to ν(OH). The peak intensity and integrated area of the ν(OH) VSB are, respectively, 0.5 and 2.5 times those of the ν_s(CO) VSB. With a ν_{exc} $\sim$32,125 cm^{-1}, which is near the peak of the ZPL for fully hydrated Gd^{3+}, the intensity of both the ν(OH) and the ν(CO) VSB of the Gd^{3+} RMPA complex are decreased to $\sim$60% of their intensities when ν_{exc} is at $\sim$32,075 cm^{-1}. The shape, position, and relative intensity of the ν(CO) bands remain essentially unchanged with variation in ν_{exc}; however, the ν(OH) band does change line shape with a change in ν_{exc}. This spectral change is characterized as a loss in relative intensity on the high shift frequency end of the ν(OH) spectral envelope when ν_{exc} is shifted to the blue. The peak position of ν(OH) shifts to $\sim$3,200 cm^{-1} and the width narrows by $\sim$80 cm^{-1}. The bulk of the ν(OH) band intensity closely follows that of the ν(CO) band with changes in ν_{exc}. When the Gd^{3+} to RMPA concentration is doubled, the intensity of the ν(OH) band increases to the level of the 1,570 cm^{-1} band. Furthermore, the position and shape of the ν(OH) band now resembles that of fully hydrated Gd^{3+}, including the presence of ν_s(OH) and ν_a(OH). A band with a significantly weaker intensity is measured at $\sim$2,945 cm^{-1}, which we assign to ν_a(CH) (28).

DOPC: phospholipid

Figs. 2 *d*, 3 *c*, 4 *a*, and 5 *b* show the VSB spectra of Gd^{3+} in a dried film of DOPC at 16°K excited at the peak of the ZPL with ν_{exc} $\sim$32,050 cm^{-1}. The peaks at shift frequencies of $\sim$1,080 and $\sim$1,200 cm^{-1} correspond closely to the symmetric (ν_s[PO] $\sim$1,090 $\pm$ 25 cm^{-1}) and anti-symmetric (ν_a[PO] $\sim$1,230 $\pm$ 10 cm^{-1}) PO stretches of phosphates in lipids measured by IR absorption (29,

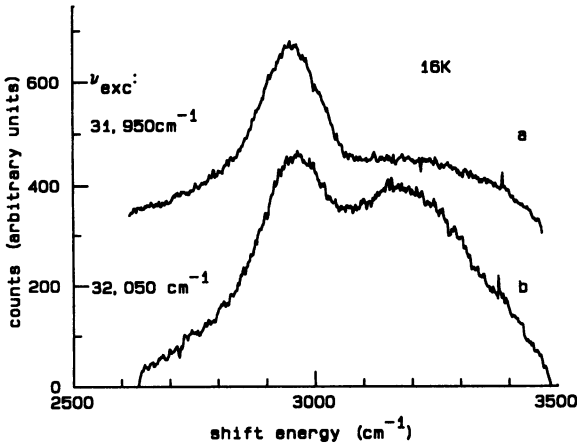

FIGURE 4 VSB fluorescence emission spectra of ~0.4 M Gd^{3+} in a dried film of the lipid DOPC at 16°K with ν_{exc} ~31,950 cm^{-1} (*a*) and ν_{exc} ~32,050 cm^{-1} (*b*). The spectra are plotted in arbitrary intensity units versus frequency shift from the average frequency of the corresponding ZPL. The time window is from 5 μs to 6 ms after the excitation pulses. The relative intensity of the peak of the VSB in *a* to that of *b* is one to three. The VSB having peaks at ~2,960 and ~3,200 cm^{-1}, respectively, correspond to ν(CH) and ν(OH).

30). In contrast, the fluorescence spectrum of inorganic phosphate buffer yields a single peak with a shift frequency of ~1,060 cm^{-1}, which corresponds to the peak at ~1,177 cm^{-1} for $\nu(PO)_s$ measured with IR

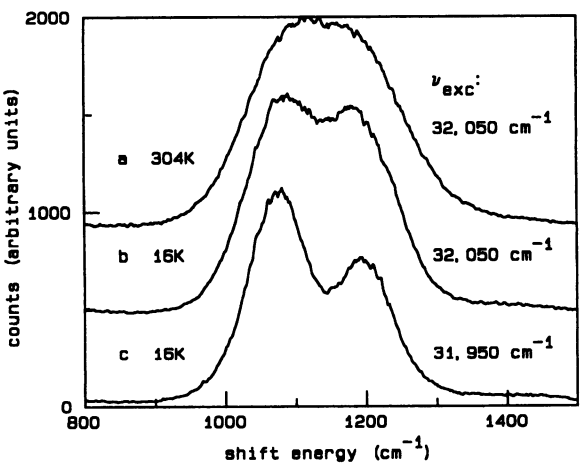

FIGURE 5 VSB fluorescence emission spectra for ν_s(PO) ~1,080 cm^{-1} and ν_a(PO) ~1,200 cm^{-1} of ~0.4 M Gd^{3+} in a dried film of the lipid DOPC at 300°K with ν_{exc} ~31,950 cm^{-1} (the spectral shape is independent of ν_{exc}) (*a*), at 16°K with ν_{exc} ~31,950 cm^{-1} (*b*) and at 16°K with ν_{exc} ~32,050 cm^{-1} (*c*). The VSB spectra are plotted in arbitrary intensity units versus frequency shift from the average frequency of the corresponding ZPL. The time window is from 5 μs to 6 ms after the excitation pulse. The relative intensity at 16°K of the ν(PO) VSB is three (*b*) to one (*c*).

absorption (30). The weak peaks at ~2,970 and ~3,200 cm^{-1} are from ν(CH) (28, 29) and ν(OH), respectively. The shape of ν(OH) is essentially that of fully hydrated Gd^{3+} and has an intensity ~10–20 times weaker than that of the PO VSB. When ν_{exc} is shifted to the red edge of the $^6P_{7/2}$ level, (ν_{exc} ~31,950 cm^{-1}), the ν(OH) band disappears while the ν(CH) band is clearly visible (Fig. 4 *b*). Also, the relative intensity of the ν_a(PO) band to the ν_s(PO) band decreases from 1:1 with ν_{exc} ~32,050 cm^{-1} (Fig. 5 *b*) to 1:1.5 with ν_{exc} ~31,950 cm^{-1} (Fig. 5 *c*). The intensity of the ν(PO) and ν(CH) VSB both decrease by about a factor of ~3 when ν_{exc} is changed from ~32,050 to ~31,950 cm^{-1}. The pronounced variation in ν_{exc} persisted to ~250°K for the Dried DOPC film. At 300°K, a single envelope for the ν(PO) VSB is observed (Fig. 5 *a*) and the marked variation in line shape with different ν_{exc} is lost.

Calf-thymus DNA

In marked contrast to the above systems, Gd^{3+} coordinated to DNA at room temperature does not yield observable VSB, and the ZPL is barely detectable. This effect is due to the strong absorption of UV light by the base pairs (31).[3] The UV absorption bands of the DNA, which are centered at 285 nm and below, narrow at cryogenic temperatures, causing their absorption at ~311 nm and 80°K to become weaker than that of Gd^{3+} (31).[3] Under these conditions the VSB are detectable. The most dominant VSB is associated with ν(OH) (not shown). The positions, relative intensities, and excitation profile of the ν_s(OH) and ν_a(OH) VSB are essentially the same as for fully hydrated Gd^{3+}. The other VSB are a factor of 10 weaker in intensity. Excitation at the peak of the ZPL (ν_{exc} = ~32,075 cm^{-1}) results in five VSB between 900 and 2,000 cm^{-1} (Fig. 6 *a*). The band at ~1,650 cm^{-1} is associated with ν_2(OH). The bands at ~1,100–1,150 and ~1,240 cm^{-1} are respectively assigned to ν_s(PO) and ν_a(PO) (32). Two other bands are observed at ~1,350 and ~1,460 cm^{-1} which could be associated with Gd^{3+} coordinated either to the buffer or

[3]Though the peak absorbance of DNA (~275 nm) is far from the $^6P_{7/2} \rightarrow {}^8S_{7/2}$ transition in Gd^{3+} (~311 nm), the absorptivity of the base pairs of DNA are ~10^4 times larger than is the absorptivity of the rare earths 4f–4f transitions. For example, in a neutral aqueous solution at room temperature, cytidine has an absorption peak ~271 nm, an absorptivity of ~9,000 M^{-1} cm^{-1}, and a fwhm of ~25 nm. Assuming a gaussian band shape for the wavelength dependence of the absorption band, the absorptivity of citidine at 311 nm would be: 9,000 exp [−(311 − 271)^2/18^2] or ~9,000 e^{-5} ~65 M^{-1} cm^{-1}. The electronic transitions of Gd^{3+} are of the order of 1 M^{-1} cm^{-1}. If the DNA absorption bands narrow by a factor of 0.73 to ~18 nm fwhm, then the absorption at 311 nm will decrease to ~1 M^{-1} cm^{-1}, and will be of the same order as the absorption by the Gd^{3+}.

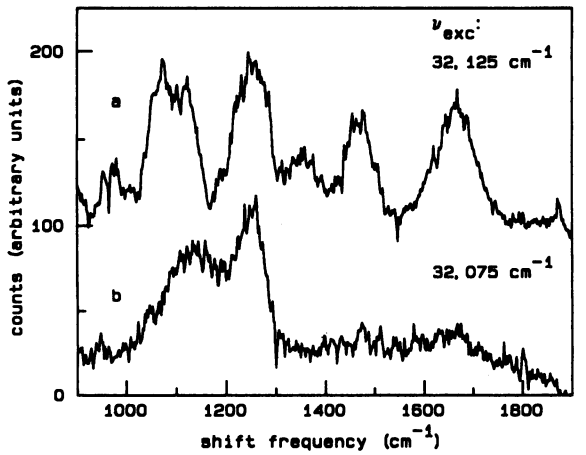

FIGURE 6 The VSB spectra of ~0.5 mM Gd^{3+} coordinated to calf-thymus DNA in H_2O at 80°K after narrow band excitations at 32,075 cm^{-1} (*a*) and 32,125 cm^{-1} (*b*). The VSB spectra are plotted in arbitrary intensity units versus frequency shift from the average frequency of the corresponding ZPL. The time window is from 5 μs to 6 ms after the excitation pulse. The relative intensity of both the ~1,240 cm^{-1} VSB and the ZPL in *a* compared to *b* is ~1.5 to 1.

to other portions of the DNA. Preliminary results with the synthetic DNAs poly(*d*A)-poly(*d*T) and poly[*d*(A–T)] indicate that these bands may not only be associated with the DNA but also could be sequence dependent. Excitation to the red edge of the ZPL (ν_{exc} = 32,125 cm^{-1}) results in a slight decrease in the intensity of the ν_s(PO) and ν_a(PO) VSB, whereas the other bands, including ν(OH), decrease significantly (Fig. 6 *b*). When the DNA precipitates out of solution due to its coordination to Gd^{3+}, the intensity of the ν(PO) and ν(OH) VSB are of approximately equal intensities for ν_{exc} ~32,125 cm^{-1}, and the ν(PO) VSB dominate the VSB spectra for all ν_{exc}. The intensity ratio of the ν_s(OH) to the ν_a(OH) modes deviates slightly and the peak position for ν(OH) shifts slightly (−20 cm^{-1}) to lower shift frequency from that of fully hydrated Gd^{3+}. These deviations from the ν(OH) spectrum of fully hydrated Gd^{3+} are minor compared to those observed for the ν(OH) bands of Gd^{3+} coordinated to EDTA or RMPA. The excitation profile for the VSB essentially follows that observed for calf-thymus DNA (*vide supra*).

DISCUSSION

H_2O; hydration layer

The nature of water in biological systems is of considerable interest and has been studied using IR spectroscopy of dehydrated films (33). VSB spectroscopy, though, yields information on the vibrational spectra of water molecules directly coordinated to the Gd^{3+} ion. To compare the ν(OH) VSB spectra from different systems, the structure of the OH VSB for fully hydrated Gd^{3+} is taken as a reference. Because fully hydrated Gd^{3+} has nine waters in its first coordination sphere (3, 34), it serves as a minihydration layer. As stated earlier, the two peaks at 3,185 and 3,325 cm^{-1} are assigned as ν_s(OH) and ν_a(OH). Though the peak position and the width of the ν(OH) VSB contain valuable information, the assignment and interpretation of the ν(OH) VSB is complicated by possible Fermi resonance of $2\nu_2$(OH) with ν_a(OH), strong intermolecular and intramolecular coupling (26), and disorder in the O-H stretching force constants (14, 35, 36). Isotopically dilute OH oscillators, ν_{uc}(OH), (i.e., small fraction of HDO in H_2O) are dynamically decoupled from their neighbors and therefore allow for a simpler ν(OH) spectrum.

A previous comparison (14) of the VSB and IR spectra of ν_{uc}(OH) at room temperature was made using isotopically dilute OH oscillators in D_2O. This study showed that the VSB peak at ~3,315 cm^{-1} is ~85 cm^{-1} lower and the fwhm of ~335 cm^{-1} is ~1.5× broader than the peak and fwhm of the IR spectrum of the bulk water. The increase in the width and the decrease in the peak position of the VSB compared to the IR spectrum, respectively, indicate that the hydrogen bonds between waters of the first and second hydration layers have a broader distribution and are on the average stronger than is the case for the hydrogen bonds between waters of the bulk liquid (14, 35, 36). The VSB spectrum of isotopically dilute OH oscillators (i.e., 3 M HDO in D_2O) measured at 80°K in this paper has a peak position of ~3,305 cm^{-1} and a fwhm of 240 cm^{-1}. These values of ν_{uc}(OH) for hydrated OH oscillators are similar to those of vitreous ice (28) where ν_{uc}(OH) ~3,310 cm^{-1} with a fwhm of ~260 cm^{-1}. Ice I (25) at ~80°K has a peak position for ν_{uc}(OH) of ~3,277 cm^{-1} and a fwhm of ~120 cm^{-1}. The waters surrounding the Gd^{3+} ions thus form an amorphous hydration layer with hydrogen bond characteristics similar to those of vitreous ice. The hydrogen bond strengths of the water molecules in the hydration layer of Gd^{3+} are weaker than those of the surrounding ice, and have a larger distribution in bond strengths.

EDTA: organic metal chelator

EDTA is used here as a model Ca^{2+} binding system because it has a high binding constant, log (*K*) ~17.4 for Gd^{3+}, and it has well characterized interactions with lanthanides (34). A single EDTA ion can contribute up to six coordination bonds with a metal ion; these bonds include two nitrogen and four oxygen bonds. Furthermore, three to four water molecules are expected to be

coordinated the Gd^{3+} (3, 34). The large intensity of ν(CO) VSB compared to the ν(OH) VSB and the difference in spectral shape of the ν(OH) VSB from that of fully hydrated Gd^{3+} indicates that the Gd^{3+} is bound to the EDTA molecule. The factor of approximately four in the integrated area of the ν(CO) VSB over the ν(OH) VSB indicates that the CO dipole moment is considerably stronger than the OH dipole of the coordinated H_2O molecules. The center of the ν(OH) band at 80°K is $\sim$85 cm^{-1} higher for waters coordinated to Gd^{3+} bound to EDTA ($\sim$3,370 cm^{-1}) than for waters of the fully hydrated Gd^{3+} complex ($\sim$3,285 cm^{-1}). This increase in the position of ν(OH) indicates that hydrogen bonds between water in the first and the second hydration layer of Gd^{3+} are longer and weaker in the Gd^{3+}·EDTA·H_2O_x complex than in the fully hydrated Gd^{3+} complex. The low intensity of the ν(CH) band is due to the fact that the CH residues in EDTA are one coordination-distance more remote from Gd^{3+} than are the carbonyls and waters.

RMPA: calcium binding protein

Parvalbumins are representative of the Kretsinger EF-hand class of Ca^{2+} binding proteins (37, 38). These proteins have two tight Ca^{2+} binding sites, one in the EF and another in the CD domain, respectively, having five and six protein donated oxygen-containing ligands coordinated to the Ca^{2+} ion (3, 37–39). X-Ray crystallographic studies suggest that the CD domain is not accessible to the solvent whereas the EF domain is, and probably has one coordinated water (3, 40). A Eu^{3+} fluorescent study (41) on carp parvalbumin indicates that the number of waters coordinated to a metal ion is one to two in the EF domain and zero to one with a serine hydroxyl group at the CD domain. At both sites, one coordinated water is given as the most likely number. The results from the present Gd^{3+} VSB study indicate that future VSB titration studies should provide the necessary detail to discriminate between conflicting claims regarding the number of coordinated water molecules at each site.

The assignment of the peaks at 1,570 and 1,460 cm^{-1} to ν_s(CO) and ν_a(CO) from carbonyls is in agreement with x-ray structures of parvalbumins (3, 37–40). The large difference in the spectral shape, the absolute position, and the excitation profile of the VSB of Gd^{3+} coordinated to RMPA compared to Gd^{3+} coordinated to EDTA indicate that the Gd^{3+} environments are distinctly different for these molecules. The increased ratio of intensity of the ν(OH) VSB to the ν(CO) VSB when the Gd^{3+} to RMPA ratio is increased beyond two to one indicates that RMPA has at most two tight binding sites for Gd^{3+}. The fact that the shape of ν(CO) remains essentially unchanged whereas the shape and position of ν(OH) resemble that of fully hydrated Gd^{3+} support this interpretation. Because the shape and position of the ν(CO) bands are relatively insensitive to ν_{exc}, the two sites must be similar. These conclusions are in agreement with H-NMR (42) and Eu^{3+} fluorescence (41, 43) studies of other parvalbumins that reveal at most two tight binding sites for Ln^{3+} with similar binding constants. The low intensity of the ν(CH) band, 2,945 cm^{-1}, can be attributed to the fact that CH groups are not directly coordinated to the Gd^{3+}.

The peak at $\sim$3,280 cm^{-1} is due to ν(OH). Because NH groups are not likely to coordinate to Gd^{3+}, the ν(OH) VSB is not complicated by interference from ν(NH) as in the case of IR spectra of proteins (33). The shape and position of the ν(OH) VSB is clearly distinct from fully hydrated Gd^{3+}, indicating that the primary source of the ν(OH) VSB is from Gd^{3+} coordinated to the protein. The broadness of the band relative to that observed for fully hydrated Gd^{3+} indicates a larger inhomogeneity in OH bond strengths (14, 25, 35, 36). This large inhomogeneity is not unexpected in proteins and has been observed in low temperature studies of heme proteins (44, 45) and in the Ca^{2+} binding protein Calmodulin (46). Furthermore, a significant portion of the ν(OH) VSB has a larger shift frequency than for fully hydrated Gd^{3+}. Because the bulk of the ν(OH) VSB intensity tracks the intensity of the ν(CO) VSB with changes in ν_{exc}, rather than the excitation profile of ν(OH) for fully hydrated Gd^{3+}, the associated waters are in the same environment as the coordinated CO molecules. As in the case of water coordinated to Gd^{3+} that is bound to EDTA, water coordinated to Gd^{3+} on the interior of the protein is expected to have an increase in the position of ν(OH) due to a disruption of the hydrogen bonding with other waters. The portion of the ν(OH) VSB on the high-frequency end of the band may also be due to a protein hydroxyl at one of the binding sites (3, 41). Because we have not acquired data for a Gd^{3+} to protein ratio of less than two-to-one, the ν(OH) signals may contain a small contribution from fully hydrated Gd^{3+}.

DOPC: phospholipid

Cations have been shown to bind to neutral phosphatidylecholines, and the coordination sites have been inferred to be to the negatively charged oxygen atoms of the phosphates (7, 8, 47, 48). Fluorescence studies (18, 47, 48) of Ln^{3+} ions coordinated to phosphatidylcholine vesicles reveal two classes of Ln^{3+} binding sites. The populations of the two Ln^{3+} · lipid coordination structures vary above and below the liquid-crystalline phase transition temperature, T_c. Above T_c, only the weak

binding site is observed. This site, which is in rapid equilibrium with fully hydrated Ln^{3+}, has only one or two waters removed from the fully hydrated Ln^{3+} ion. It is suggested that the Ln^{3+} is coordinated to the negatively charged oxygen of a single phosphate moiety. Below T_c, the population of the weak binding site decreases substantially, while a new tight binding site appears. The Ln^{3+} at the tight binding site is more dehydrated, having one, or at most two, water molecules coordinated to it. It is suggested that for these sites the Ln^{3+} is coordinated to two neighboring phosphates.

The VSB spectra measured in this paper yield direct information on Ln^{3+} coordination sites in phosphatidylcholines. The intense ν(PO) VSB show that the predominant Ln^{3+} ligand is the phosphate of the lipid head group. The relative intensities of the symmetric to the antisymmetric vibrations are known (29, 30, 49) to be altered by the symmetry and coordination structure of the molecular environment. The dramatic difference in the relative intensity of the ν_s(PO) to the ν_a(PO) VSB with changes in ν_{exc} measured at cryogenic temperatures (up to 250°K) indicates that the Gd^{3+} ion which is coordinated to the phosphates of DOPC can be in at least two different phosphate environments below T_c. The similarity in the shape and position of ν(OH) with that of fully hydrated Gd^{3+} with ν_{exc} near the peak of the ZPL indicates that either the ν(OH) VSB is from fully hydrated Gd^{3+} or that the phosphate environment of the lipid does not significantly disrupt the hydrogen bonding of the waters in the Gd^{3+}·DOPC·H_2O_x complex. The disappearance of the ν(OH) band with red edge excitation of the ZPL indicates that the sites excited with these frequencies are relatively dehydrated. This dehydrated environment might correspond to the tight binding structure. At cryogenic temperatures, the environment of a Gd^{3+} ion cannot fluctuate within the fluorescence time scale. Thus, the different binding sites can be preferentially excited. The disappearance of site selectivity at 300°K indicates that the Gd^{3+} is in rapid exchange (submillisecond exchange rates) between the two phosphate environments, and the ensemble average of the Gd^{3+} environments is probed.

Calf-thymus DNA

The presence of the ν(PO) band in the VSB spectra of Gd^{3+} coordinated to DNA indicates that Gd^{3+} is coordinated to the phosphates of the DNA, as is expected from electrostatic arguments. The increase in intensity of the ν(PO) VSB when the Gd^{3+}·DNA complex precipitates out of solution indicates that it is the coordination of the trivalent ion to the phosphates that causes the precipitation. A titration study by Yonuschot et al. (50) of the precipitate of Tb^{3+} coordinated to calf-thymus DNA showed that one Tb^{3+} per phosphate group coordinates to the DNA. If each Gd^{3+} coordinates to a single phosphate group, then multiple waters should also be coordinated to the Gd^{3+}, which could explain the large intensity of the ν(OH) VSB seen in the precipitate. The large difference in the intensity of the ν(OH) and the ν(PO) VSB with different ν_{exc}, though, indicates that at least two Gd^{3+} coordination structures exist which have different amounts of coordinated phosphates and waters. One possible environment is fully hydrated Gd^{3+}. Another possibility is the existance of different complexes having either a 1:1 or a 1:2 Gd^{3+} to phosphate coordination number. The temperature difference in our study from that of Yonushot et al. (50) could allow for the existence of a coordination structure other than the 1:1 Gd^{3+} to phosphate observed by Yonuschot et al. (50). The change in the intensity ratio of the ν_s(OH) VSB to the ν_a(OH) VSB observed in the precipitate compared to fully hydrated Gd^{3+} indicates that a significant fraction of the ν(OH) VSB observed in the DNA precipitate are from waters coordinated to the Gd^{3+}·DNA complex rather than from waters of fully hydrated Gd^{3+}. The similarity in the position (< 25 cm^{-1} shift) and width (essentially identical) of the ν(OH) VSB spectra for the waters coordinated to the Gd^{3+}·DNA complex with those of fully hydrated Gd^{3+} is consistant with IR studies of DNA (33, 51) that indicate that water coordinated to DNA has a broad distribution of OH bond strengths, and does not crystallize upon cooling to cryogenic temperatures.

X-Ray studies of DNA indicate that metal ions can coordinate to carbonyls in the major or minor grooves under the appropriate electrostatic and stereochemical conditions (52). The 1,350 and 1,460 cm^{-1} bands might be from Gd^{3+} coordinated to molecular groups other than phosphates. Weak bands at these positions are observed in IR studies (32) and are expected to be from NH or CH in-plane deformation vibrations in the base residues. The weakness of these bands in the VSB spectra, though, does not yield compelling evidence for a significant fraction of the Gd^{3+} ions being coordinated to molecular groups other than phosphates or waters. The strong IR active C = O vibrations between ~1,600 and 1,700 cm^{-1} are not observed to any significant degree in our Gd^{3+} VSB studies.

CONCLUSION

The results presented in this article show that the VSB fluorescence of Gd^{3+} coordinated to biomolecules can be used for determining structural information localized to the metal ion's coordination sites. We have directly measured site specific vibrational spectra for molecular

ligands coordinated to Gd^{3+} in a Ca^{2+} binding protein, a lipid head group, an organic metal chelator, and DNA. These data are not obscured by the rich infrared spectra of these samples. Instead, they reflect the vibrational frequency of molecular groups in the immediate environment about the Gd^{3+}. This feature is due to: the fluorescence being in the UV, the VSB phenomenon resulting from a short-range force, and the ability to remove Raman signals by the gating technique. The combination of the long excited state lifetime for Gd^{3+}, and the site specificity of the VSB via changes in ν_{exc} allow for the determination of localized structure and dynamics within complex systems containing multiple Ca^{2+} binding sites. This paper represents the first attempt at determining the capabilities of this new technique for use in biological samples.

The authors would like to thank E. Shyamsunder for preparing the lipid sample and for helpful comments, and R. Austin for advice in the preparation of the DNA and other beneficial comments. Both are from the Physics Department of Princeton University.

Received for publication 21 September 1990 and in final form 21 December 1990.

REFERENCES

1. Martin, R. B., and F. S. Richardson. 1979. Lanthanides as probes for calcium in biological systems. *Q. Rev. Biophys.* 12:181–209.
2. Horrocks, W. DeW., Jr. 1982. Lanthanide ion probes of biomolecular structure. *Adv. Inorg. Biochem.* 4:201–261.
3. Horrocks, W. DeW., Jr., and D. R. Sudnick. 1981. Lanthanide ion luminescence probes of the structure of biological macromolecules. *Acc. Chem. Res.* 14:384–392.
4. Horrocks, W. DeW., Jr., and W. E. Collier. 1981. Lanthanide ion luminescence probes. Measurement of distance between intrinsic protein fluorophores and bound metal ions: quantitation of energy transfer between tryptophan and terbium(III) or europium(III) in the calcium-binding protein parvalbumin. *J. Am. Chem. Soc.* 103:2856–2862.
5. Mulqueen, P., J. M. Tingey, and W. DeW. Horrocks, Jr. 1985. Characterization of lanthanide(III) ion binding to calmodulin using luminescence spectroscopy. *Biochemistry.* 24:6639–6645.
6. Bentz, J., D. Alford, J. Cohen, and N. Düzgünes. 1988. La^{3+}-induced fusion of phosphatidylserine liposomes. *Biophys. J.* 53:593–607.
7. Chrzeszczyk, A., A. Wishnia, and C. S. Springer, Jr. 1981. Evidence for cooperative effects in the binding of polyvalent metal ions to pure phosphatidylcholine bilayer vesicle surfaces. *Biochim. Biophys. Acta.* 648:28–48.
8. Grasdalen, H., L. E. G. Eriksson, J. Westman, and A. Ehrenberg. 1977. Surface potential effects on metal ion binding to phosphatidylcholine membranes: ^{31}P NMR study of lanthanide and calcium ion binding to egg-yolk lecithin vesicles. *Biochim. Biophys. Acta.* 469:151–162.
9. Ewald, Von H. 1939. Die analyse und deutung der neodymsalzspektren. *Ann. d. Physik.* 34:209–236.
10. Freed, S. 1942. IV spectra of ions in crystals and solutions. *Rev. Mod. Phys.* 14:105–111.
11. Stavola, M., L. Isganitis, and M. G. Sceats. 1981. Cooperative vibronic spectra involving rare earth ions and water molecules in hydrated salts and dilute aqueous solutions. *J. Chem. Phys.* 74:4228–4241.
12. Faulkner, T. R., and R. S. Richardson. 1978. Vibronic coupling model for the intensities of f–f transitions in octahedral lanthenide(III) complexes. *Mol. Physics.* 35:1141–1161.
13. Yatsiv, S., E. Ehrenfreund, and U. El-Hanany. 1965. Internal vibronics in terbium compounds—A cooperative phenomenon. *J. Chem. Phys.* 42:743–749.
14. Stavola, M., J. M. Friedman, R. A. Stepnoski, and M. G. Sceats. 1981. Hydrogen bonding between solvation shells around Gd^{3+} from cooperative vibrionic spectra. *Chem. Phys. Lett.* 80:192–194.
15. Macgregor, R. B., Jr. 1989. Vibrational spectroscopy in the ultraviolet via Gd^{3+} fluorescence: application to biological systems. *Arch. Biochem. Biophys.* 274:312–316.
16. Hall, D. W., S. A. Brawer, and M. J. Weber. 1982. Vibronic spectra of Gd^{3+} in metaphosphate glasses: comparison with raman and infrared spectra. *Phys. Rev.* B25:2828–2837.
17. Brecher, C., and L. A. Riseberg. 1980. Laser-induced linenarrowing of Eu^{3+} fluorescence in fluoroberyllate glass: site-dependent spectroscopic properties and their structural implications. *Phys. Rev.* B21:2607–2618.
18. Halladay, H. N., and M. Petersheim. 1988. Optical properties of Tb^{3+}-phospholipid complexes and their relation to structure. *Biochemistry.* 27:2120–2126.
19. Herrmann, T. R., A. R. Jayaweera, and A. E. Shamoo. 1986. Interaction of europium(III) with phospholipid vesicles as monitored by laser-excited europium(III) luminescence. *Biochemistry.* 25:5834–5838.
20. Spiro, T. G., Editor. 1988. Biological Applications of Raman Spectroscopy. Vol. 3. John Wiley & Sons, Inc., New York. 556 pp.
21. Carnall, W. T., P. R. Fields, and K. Rajnak. 1968. Electronic energy levels of trivalent lanthanide aquo ions. II. Gd^{3+}. *J. Chem. Physics.* 49:4443–4446.
22. Haas, Y., G. Stein, and E. Würzberg. 1973. Temperature effects on radiative and radiationless transitions of Gd^{3+} in solution. *J. Chem. Phys.* 58:2777–2780.
23. Lehky, P., H. E. Blum, E. A. Stein, and E. H. Fischer. 1975. Isolation and characterization of parvalbumins from the skeletal muscle of higher vertebrates. *J. Biol. Chem.* 249:4332–4334.
24. Stavola, M., and D. L. Dexter. 1979. Energy transfer and two-center optical transitions involving rare-earths and OH-impurities in condensed matter. *Phys. Rev.* B20:1867–1885.
25. Bertie, J. E., and E. Whalley. 1964. Infrared spectra of ices Ih and Ic in the range 4000 to 350 cm^{-1}. *J. Chem. Phys.* 40:1637–1645.
26. Eisenberg, D., and W. Kauzmann. 1969. The Structure and Properties of Water. Oxford University Press, New York.
27. Kolat, R. S., and J. E. Powell. 1962. The solid rare earth chelates of ethylenediaminetetraacetic acid. *Inorg. Chem.* 1:485–490.
28. Snyder, R. G., H. L. Strauss, and C. A. Elliger. 1982. C-H stretching modes and the structure of *n*-alkyl chains. 1. Long, disordered chains. *J. Phys. Chem.* 86:5145–5150.
29. Dluhy, R. A., D. G. Cameron, H. H. Mantsch, and R. Mendelsohn. 1983. Fourier transform infrared spectroscopic studies of the effect of calcium ions on phosphatidylserine. *J. Biochem. (Tokyo).* 22:6318–6325.

30. Arrondo, J. L. R., F. M. Goñi, and J. M. Macarulla. 1984. Infrared spectroscopy of phosphatidylcholines in aqueous suspension. A study of the phosphate group vibrations. *Biochim. Biophys. Acta.* 794:165–168.

31. Bloomfield, V. A., D. M. Crothers, and I. Tinoco, Jr. 1974. Physical Chemistry of Nucleic Acids. Harper & Row, New York. 24 pp.

32. Sutherland, G. B. B. M., F. R. S. Tsuboi, and M. Tsuboi. 1957. The infrared spectrum and molecular configuration of sodium deoxiribonucleate. *Proc. R. Soc. Edinb. Sect. A. (Math. Phys. Sci.).* A239:446–463.

33. Kuntz, I. D., Jr., and W. Kauzmann. 1974. Hydration of proteins and polypeptides. *Adv. Protein Chem.* 28:239–345.

34. Gschneidner, K. A., and L. R. Eyring, Editors. 1979. The Handbook on the Physics and Chemistry of Rare Earths. Vol. 3. North-Holland Publishing Co., Amsterdam.

35. Falk, M. 1975. Vibrational Band Profiles and the Structure of Water and of Aqueous Solutions. *In* The Proceedings of the Electrochemical Society Symposium on Chemistry and Physics of Aqueous Solutions. Electrochemical Society, Toronto, Canada. 19–41.

36. Wall, T. T., and D. F. Hornig. 1965. Raman intensities of HDO and structure in liquid water. *J. Chem. Phys.* 43:2079–2087.

37. Kretsinger, R. H. 1980. Structure and evolution of calcium-modulated proteins. *CRC Crit. Rev. Biochem.* 8:119–174.

38. Kretsinger, R. H. 1976. Calcium Binding Proteins. *A. Rev. Biochem.* 45:239–266.

39. Kretsinger, R. H., and C. E. J. Nockolds. 1973. Carp muscle calcium-binding protein: II. Structure determination and general description. *J. Biol. Chem.* 248:3313–3326.

40. Sowadsky, J., G. Cornick, and R. H. Kretsinger. 1978. Terbium replacement of calcium in parvalbumin. *J. Mol. Biol.* 124:123–132.

41. Moo-Jhong, R., D. R. Sudnick, V. K. Arkle, and W. DeW. Horrocks, Jr. 1981. Lanthanide ion luminescence probes. Characterization of metal ion binding sites and internal energy transfer distance measurements in calcium-binding proteins. I. Parvalbumin. *Biochemistry.* 20:3328–3334.

42. Williams, T. C., D. C. Corson, and B. D. Sykes. 1984. Calcium-binding proteins: Calcium(II)–lanthanide(III) exchange in carp parvalbumin. *J. Am. Chem. Soc.* 106:5698–5702.

43. Breen, P. J., E. K. Hild, and W. DeW. Horrocks, Jr. 1985. Spectroscopic studies of metal ion binding to tryptophan-containing parvalbumin. *Biochemistry.* 24:4991–4997.

44. Iben, I. E. T., D. Braunstein, W. Doster et al. 1989. Glassy behavior of a protein. *Phys. Rev. Lett.* 62:1916–1919.

45. Ormos, P., A. Ansari, D. Braunstein, B. R. Cowen, H. Frauenfelder, M. K. Hong, I. E. T. Iben, T. B. Sauke, P. J. Steinbach, and R. D. Young. 1990. Inhomogeneous broadening in spectral bands of carbonmonoxymyoglobin: the connection between spectral and functional heterogeneity. *Biophys. J.* 57:191–199.

46. Austin, R. H., D. L. Stein, and J. Wang. 1987. Terbium luminescence lifetime heterogeneity and protein equilibrium conformational dynamics. *Proc. Natl. Acad. Sci. USA.* 84:1541–1545.

47. Cader, B. M., and W. DeW. Horrocks, Jr. 1988. A laser-induced europium(III) ion luminescence study of the interaction of this ion with phospholipid bilayer vesicles above and below the gel to liquid-crystalline phase transition temperature. *Biophys. Chem.* 32:97–109.

48. Conti, J., H. N. Halladay, and M. Petersheim. 1987. An ionotropic phase transition in phosphatidylcholine cation and anion cooperativity. *Biochim. Biophys. Acta.* 902:53–64.

49. Decius, T. C., and R. M. Hexter. 1977. Molecular Vibrations in Crystals. McGraw-Hill, Inc., New York.

50. Yonuschot, G., and G. W. Mushrush. 1975. Terbium as a fluorescent probe for DNA and chromatin. *Biochemistry.* 14:1677–1681.

51. Falk, M., A. G. Poole, and C. G. Goymour. 1970. Infrared study of the state of water in the hydration shell of DNA. *Can. J. Chem.* 48:1536–1542.

52. Rosenberg, J. M., N. C. Seeman, J. J. Park Kim, F. L. Suddath, H. B. Nicholas, and A. Rich. 1973. Double helix at atomic resolution. *Nature (Lond.).* 243:150–154.